

Bandwidth Studies on Multimode Polymer Waveguides for ≥ 25 Gb/s Optical Interconnects

Nikolaos Bamiedakis, Jian Chen, Richard V. Penty, *Senior Member, IEEE*, and Ian H. White, *Fellow, IEEE*

Abstract—Multimode polymer waveguides constitute a promising technology for use in board-level optical interconnects. However, the continuous improvements in high-speed performance of VCSELs raise important questions about their ability to support such high data rates due to their inherent highly multimoded nature. Thorough experimental studies on the bandwidth of a 1.4-m-long multimode spiral waveguide are presented in this letter, indicating a bandwidth-length product of at least $35 \text{ GHz} \times \text{m}$ even in the case of an overfilled launch. No significant transmission impairments are observed for spatial input offsets, while error-free ($\text{BER} < 10^{-12}$) data transmission over the 1.4-m-long spiral waveguide is demonstrated at 25 Gb/s.

Index Terms—Polymer waveguides, multimode waveguides, waveguide bandwidth, board-level optical interconnects.

I. INTRODUCTION

THE ever increasing demand in recent years for interconnection bandwidth in data centres and supercomputers, in conjunction with the inherent disadvantages of copper interconnects when operating at high data rates ($> 10 \text{ Gb/s}$), has led to the consideration of the use of optical technologies in very short communication links [1], [2]. Optics can offer higher bandwidth, reduced power consumption, increased interconnection density and relaxed thermal management requirements [3], [4]. Multimode polymer waveguides are a particularly attractive technology for use in board-to-board and module-to-module communications as they exhibit favourable optical, mechanical and thermal properties [5], [6] allowing their direct integration onto low-cost printed circuit boards (PCBs) with standard methods of conventional electronics manufacturing. The use of large waveguide dimensions ($\sim 30\text{--}70 \mu\text{m}$) offers relaxed alignment tolerances in the formation of the opto-electronic (OE) PCBs enabling board assembly with common pick-and-place tools [7], [8]. Large numbers of high-capacity board-level optical interconnects have been demonstrated using large waveguide arrays in conjunction with the use of high-speed VCSEL and PD arrays [9], [10]. The continuous improvements in the reliable operation of VCSELs at high data rates ($> 25 \text{ Gb/s}$) [11], [12] and the recent successful demonstration of non-return-to-zero (NRZ) data transmission at data rates up to 64 Gb/s with directly-modulated devices [13], raise however important questions on the bandwidth performance of multimode polymer waveguides and

their capability to support such high data rates. Some relevant bandwidth studies have been reported in the past [14]–[16], but these either examine the waveguide bandwidth only under a restricted input launch [14], [15] or focus on graded-index waveguides [16]. Moreover, the demonstration of high-speed data transmission over multimode polymer waveguides at rates up to 25 Gb/s has been limited to relatively short straight waveguides with lengths in the range of 10 to 20 cm [17], [18].

In this letter therefore, we present thorough experimental bandwidth studies on a relatively long multimode polymer spiral waveguide under different launch conditions and in the presence of spatial input offsets, and report record error-free ($\text{BER} < 10^{-12}$) data transmission at 25 Gb/s over a 1.4 m long spiral waveguide. This highly-multimoded waveguide has a cross section of $50 \times 20 \mu\text{m}^2$ and a numerical aperture (NA) of ~ 0.25 at 850 nm. The results demonstrate a bandwidth-length product of at least $35 \text{ GHz} \times \text{m}$, indicating the potential of this technology in optical interconnects at data rates beyond 25 Gb/s . In the sections that follow, the multimode polymer 1.4 m long spiral waveguide is presented (section II), the frequency response and offset launch measurements (section III) and the data transmission experiments (section IV) carried out on the waveguide are reported. Section V provides the conclusions.

II. MULTIMODE POLYMER 1.4 m LONG SPIRAL WAVEGUIDE

The work presented herein is based on multimode waveguides fabricated from siloxane polymer materials. These materials provided by Dow Corning [Dow Corning® OE-4140 (core) and OE-4141 (cladding) Cured Optical Elastomers] exhibit the required optical, mechanical and thermal properties for direct integration onto PCBs [6]. They exhibit low loss of $\sim 0.04 \text{ dB/cm}$ at the 850 nm datacommunications wavelength, they can withstand the high temperature environments in excess of $250 \text{ }^\circ\text{C}$ required for solder reflow and possess the essential environment stability to withstand normal operation of high performance electronic systems. The refractive index of the core and cladding materials are approximately 1.52 and 1.50 respectively at 850 nm. The spiral waveguide used in this work is fabricated from the siloxane polymer materials on a 6-inch glass wafer with conventional photolithography. The waveguide has a cross section of approximately $50 \times 20 \mu\text{m}^2$ while the waveguide facets are exposed with a dicing saw. No polishing steps are undertaken to improve the roughness on the input and output waveguide facets. Fig. 1 shows a photograph of the 1.4 m long waveguide illuminated with red light and an image of the waveguide output facet. The asymmetry in the waveguide core dimension is due to the limitation in the maximum achievable thickness of the core layer imposed by the viscosity of the core material solution and substrate size used in the sample fabrication. Waveguides with a larger height can however be fabricated by appropriately formulating the material solution.

Manuscript received May 13, 2014; revised July 12, 2014; accepted July 21, 2014. Date of publication July 25, 2014; date of current version September 16, 2014. This work was supported by the Engineering and Physical Sciences Research Council of U.K. through the Cambridge Integrated Knowledge Centre.

The authors are with the Department of Electrical Engineering Division, University of Cambridge, Cambridge CB2 1TN, U.K. (e-mail: nb301@cam.ac.uk; jc791@cam.ac.uk; rvp11@cam.ac.uk; ihw3@cam.ac.uk).

Color versions of one or more of the figures in this letter are available online at <http://ieeexplore.ieee.org>.

Digital Object Identifier 10.1109/LPT.2014.2342881

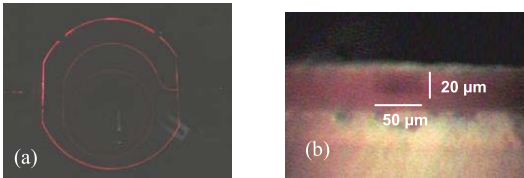


Fig. 1. Images of (a) the 1.4 m long spiral waveguide illuminated with red light and (b) the output facet of the waveguide.

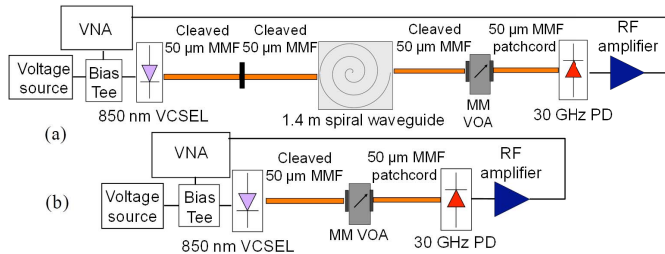


Fig. 2. Experimental setup used in the S_{21} measurement for (a) the waveguide link and (b) the back-to-back link when a typical $50/125 \mu\text{m}$ input is used.

III. EXPERIMENTAL RESULTS

The 1.4 m long spiral waveguide is employed to assess the bandwidth performance of real-world multimode polymer waveguide links.

A. S_{21} Measurements

To obtain the frequency response of the 1.4 m long spiral waveguide, the S_{21} parameter is measured for the link with and without (i.e. the back-to-back link) the spiral waveguide. The response of the spiral waveguide can be obtained by calculating the difference between the two S_{21} responses. The measurement is repeated for different launch conditions into the waveguide: i) $9/125 \mu\text{m}$ SMF launch, ii) a typical $50/125 \mu\text{m}$ OM3 MMF launch (NA of 0.2), iii) a quasi-overfilled $50/125 \mu\text{m}$ OM3 MMF launch and iv) a $100/140 \mu\text{m}$ MMF launch (NA of 0.29). The order of the different launches as quoted above corresponds to an increasing uniformity for the mode power distribution at the waveguide input and therefore, increasing levels of expected multimode dispersion in the waveguide. The employed launch conditions, although strictly-speaking not worst-case, cover a wide range of input conditions that can be encountered in real-world systems providing therefore a useful insight in the bandwidth performance of such waveguide structures. Moreover, for each type of launch, the waveguide frequency response is obtained for different positions of the input fibre in order to assess any changes in waveguide bandwidth performance due to the induced input spatial offsets. Different input positions result in different mode power distributions at the waveguide input and therefore, different levels of induced multimode dispersion.

The experimental setup employed is shown in Fig. 2. A vector network analyser (Agilent 8722ET) is connected to the 850 nm VCSEL (bandwidth ~ 25 GHz) [11] via a high-frequency RF probe. A cleaved fibre patchcord (SMF or $50/125 \mu\text{m}$ OM3 MMF or $100/140 \mu\text{m}$ MMF) is used to collect the emitted light from the VCSEL device. A cleaved fibre of the same type is employed to couple the light into the spiral waveguide. For the quasi-overfilled $50 \mu\text{m}$ MMF launch, a mode scrambler (Newport FM-1) is employed before the waveguide input to generate a more uniform mode power

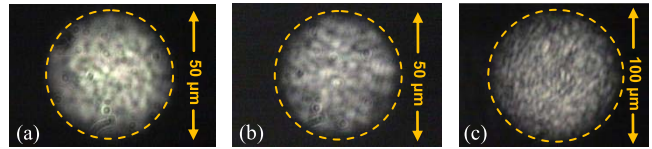


Fig. 3. Near field images of the output facet of the fibre employed to launch light into the spiral waveguide: (a) typical $50/125 \mu\text{m}$ MMF, (b) quasi-overfilled $50/125 \mu\text{m}$ MMF and (c) $100/140 \mu\text{m}$ MMF.

distribution inside the input fibre. The output of the different MMFs used at the waveguide input are imaged using a microscope objective and a camera and are shown in Fig. 3. The images show a relatively uniform power distribution over the fibre cross section for the quasi-overfilled $50 \mu\text{m}$ MMF and the $100 \mu\text{m}$ MMF launches. The input fibre is mounted on a precision translational stage in order to introduce horizontal offsets, while a displacement sensor is used to control the induced spatial offsets. At the waveguide output, a $50 \mu\text{m}$ MMF cleaved fibre collects the output light and delivers it to the high-speed PD (VIS D30-850M), while a RF amplifier is used to amplify the received electrical signals. Index matching gel is employed at both the waveguide input and output facets to minimise Fresnel losses and any scattering losses due to facet surface roughness. It should be noted that the use of the $50 \mu\text{m}$ OM3 MMF at the waveguide output, although not ideal for the dispersion measurements due to its slightly smaller NA than that of the waveguide, cannot be avoided as both the multimode variable optical attenuator (MM VOA) and high-bandwidth PD used in the link have $50 \mu\text{m}$ OM3 fibre-coupled inputs.

The total insertion loss of the spiral waveguide (including coupling losses and propagation losses) is measured to be 11.5 dB, 16.3 dB, 23.5 dB and 26.3 dB for a well-aligned SMF, $50 \mu\text{m}$ MMF, quasi-overfilled $50 \mu\text{m}$ MMF and $100 \mu\text{m}$ MMF input respectively. The main loss component in the waveguide is the bending loss due to the long waveguide bends and the inflection point at the centre of the spiral. For the back-to-back link a MM VOA (Agilent NA7766A) is employed to adjust the received optical power to levels similar to those obtained in the waveguide link. Fig. 4 shows the obtained normalised waveguide frequency response for the different input offsets. It can be observed that for all input types a flat frequency response is achieved up to at the least the 25 GHz instrumentation limit. Even in the case of the $100 \mu\text{m}$ MMF launch no significant bandwidth degradation is noticed in the link. The result demonstrates a bandwidth-length product of at least $35 \text{ GHz}\times\text{m}$ for the specific waveguide, indicating that data transmission beyond 25 Gb/s could be achieved.

B. Offset Launch Studies

A similar setup as the one shown in Fig. 2(a) is employed to carry out offset launch measurements on the 1.4 m long spiral waveguide. The VCSEL is directly modulated using an Anritsu pattern generator (MP1800A) with a long (256 bits) pattern with a single '1' bit (i.e. 000...010...000) in order to emulate the transmission of a single pulse in the waveguide. The same launch conditions as the ones used for the S_{21} measurements are employed and again spatial offsets are introduced to induce different amounts of multimode dispersion in the waveguide. The received waveform at the waveguide output for each input position is recorded with a digital communication analyser (Agilent Infiniium 86100A) and the respective received optical power is also measured.

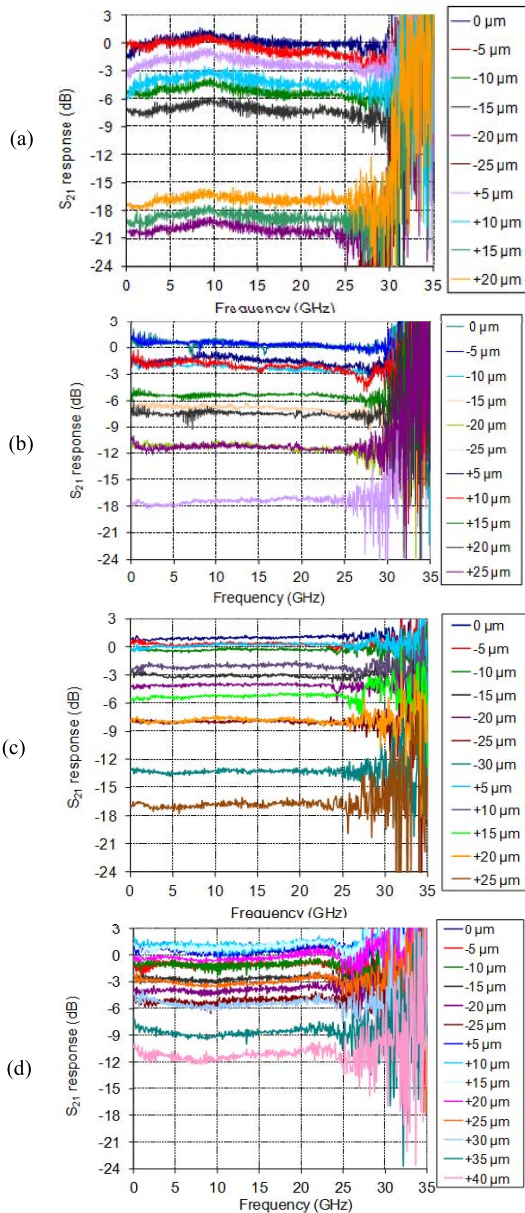


Fig. 4. Normalised frequency response for the 1.4 m long spiral waveguide for the different input positions for (a) a SMF, (b) a typical $50\ \mu\text{m}$ MMF, (c) a quasi-overfilled $50\ \mu\text{m}$ MMF and (d) a $100\ \mu\text{m}$ MMF input.

The full-width-at-half-maximum (FWHM) of the received pulse is measured for each input type and for different input positions and is plotted in Fig. 5. The plots also show the variation of the received optical power for the same input offsets. The FWHM of the pulse received in the back-to-back link is also recorded and is found to be ~ 28 ps. The results show that no significant change occurs in the pulse width for the different input offsets, demonstrating that the induced dispersion in the waveguide is very small.

The large bandwidth of the spiral waveguide observed even under relatively overfilled launch conditions can be mainly attributed to its structure. The long waveguide bends result in the suppression of higher order modes and therefore in reduced multimode dispersion at the waveguide output. Moreover, it is believed that the waveguide does not have a strict step-index profile due to the diffusion of cladding monomers during the waveguide fabrication. As a result, some variation of the refractive index profile of the waveguide core occurs near

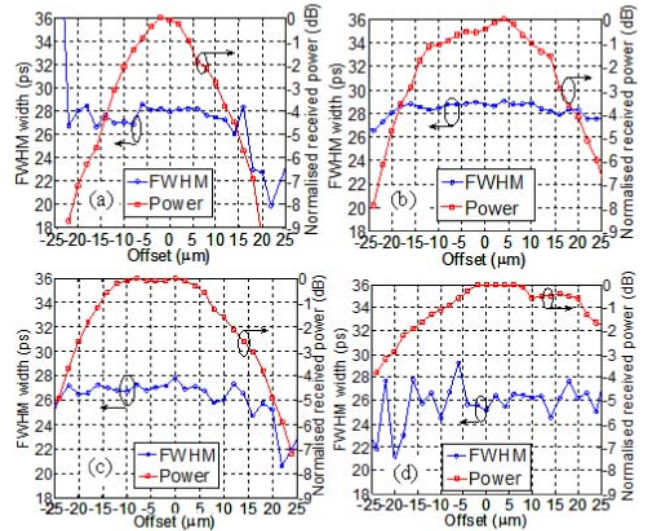


Fig. 5. Variation of the FWHM of the received pulse and received optical power after transmission over the 1.4 m long spiral waveguide for different horizontal offsets for (a) a SMF, (b) a typical $50\ \mu\text{m}$ MMF, (c) a quasi-overfilled $50\ \mu\text{m}$ MMF and (d) a $100\ \mu\text{m}$ MMF input.

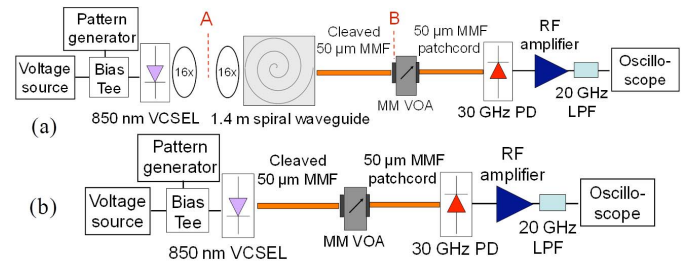


Fig. 6. Setup of the (a) waveguide and (b) back-to-back link in the data transmission experiments.

the waveguide edges resulting in a smaller numerical aperture and therefore, reduced multimode dispersion. A similar effect has been observed in other multimode waveguides produced from the same materials. Detailed refractive index studies are underway to investigate the validity of the assumption.

IV. DATA TRANSMISSION

Data transmission experiments at 20 Gb/s and 25 Gb/s are carried out on the 1.4 m long spiral waveguide. A similar setup as the one used for the S_{21} measurements is employed (Fig. 6). The VCSEL is directly modulated by a $2^7 - 1$ pseudorandom bit sequence (PRBS) to emulate the short patterns typically used in datacommunication links (e.g. 8B10B). The operating conditions of the VCSEL ($I_{\text{bias}} = 13$ mA, $V_{\text{RF}} = 1.03$ V pp) are appropriately adjusted to optimise link performance. The light is launched in the waveguide with a pair of $16\times$ microscope objectives (NA = 0.32) in order to maximise the received optical power at the PD end. The total insertion loss of the waveguide in the link is 13.2 dB [power difference between points A and B in Fig. 6(a)]. A 20 GHz RF filter is used at receiver end to minimise the received high frequency noise. The received eye diagrams are captured with the digital communication analyser and are shown in Fig. 7(a). The respective eye diagrams for the back-to-back link [Fig. 6(b)] are recorded for similar levels of received optical power and are shown in Fig. 7(b) for comparison. Open eye diagrams are recorded for

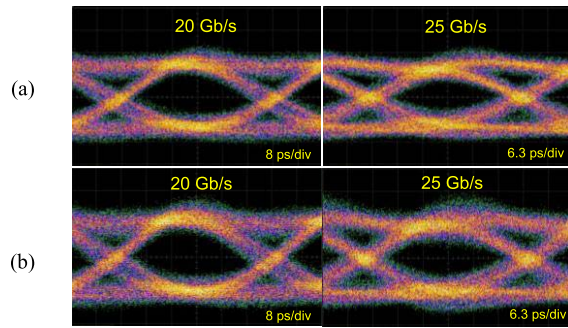


Fig. 7. Received eye diagrams at 20 Gb/s and 25 Gb/s for (a) the back-to-back link and (b) the waveguide link. Voltage scale: 25 mV/div for all eye diagrams.

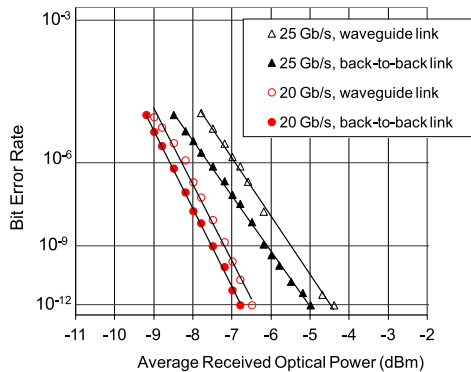


Fig. 8. BER curves for the waveguide and back-to-back links at 20 and 25 Gb/s.

the waveguide link at both data rates, while minimum signal degradation (eye closure, jitter, additional noise) is observed with the insertion of the spiral waveguide in the link.

Bit-error-rate (BER) measurements are carried out on the back-to-back and waveguide link using a BER test set (Anritsu MP1800A). Error-free ($\text{BER} < 10^{-12}$) data transmission over the 1.4 m long multimode polymer waveguide is achieved at both 20 Gb/s and 25 Gb/s. The MM VOA is inserted in the link to adjust the received optical power at the PD and record the respective BER. The obtained BER curves as a function of the average received optical power at both data rates and for both the back-to-back and waveguide link are shown in Fig. 8. The gap in the data points for the waveguide link at 25 Gb/s is due to the insertion loss of the MM VOA (~ 1.5 dB). The power penalty for a BER of 10^{-12} due to the insertion of the spiral waveguide in the link is 0.2 dB and 0.5 dB for 20 Gb/s and 25 Gb/s respectively. The results clearly demonstrate the potential use of the waveguides in board-level interconnects for transmission of at least 25 Gb/s data signals.

V. CONCLUSIONS

Multimode polymer waveguides constitute an attractive technology for use in board-level optical interconnects. Due to the highly-multimoded nature of the waveguides typically used in such applications (waveguide width: 30-70 μm , NA: 0.2-0.3) and the continuous improvements in active devices (VCSELs), important questions regarding the bandwidth performance of such waveguides are raised. S_{21} measurements on a 1.4 m long spiral waveguide demonstrate a flat frequency response up to at least 25 GHz, indicating a record

bandwidth-length product of at least 35 GHz \times m. Error-free ($\text{BER} < 10^{-12}$) data transmission is achieved at 25 Gb/s with a small power penalty of ~ 0.5 dB. The bandwidth studies and data transmission experiments indicate that the waveguides are suitable for operation at data rates of at least 25 Gb/s, while higher data rates could also be achieved.

ACKNOWLEDGMENTS

The authors acknowledge Dow Corning Corporation for the provision of the polymer samples and Chalmers University for the provision of the high-speed VCSEL devices.

REFERENCES

- [1] A. F. Benner, M. Ignatowski, J. A. Kash, D. M. Kuchta, and M. B. Ritter, "Exploitation of optical interconnects in future server architectures," *IBM J. Res. Develop.*, vol. 49, nos. 4-5, pp. 755-775, Jul. 2005.
- [2] M. A. Taubenblatt, "Optical interconnects for high-performance computing," *J. Lightw. Technol.*, vol. 30, no. 4, pp. 448-457, Feb. 15, 2012.
- [3] D. A. B. Miller, "Rationale and challenges for optical interconnects to electronic chips," *Proc. IEEE*, vol. 88, no. 6, pp. 728-749, Jun. 2000.
- [4] D. Huang, T. Sze, A. Landin, R. Lytel, and H. L. Davidson, "Optical interconnects: Out of the box forever?" *IEEE J. Sel. Topics Quantum Electron.*, vol. 9, no. 2, pp. 614-623, Mar./Apr. 2003.
- [5] M. P. Immonen, M. Karppinen, and J. K. Kivilahti, "Investigation of environmental reliability of optical polymer waveguides embedded on printed circuit boards," *Microelectron. Rel.*, vol. 47, nos. 2-3, pp. 363-371, 2007.
- [6] J. V. DeGroot, Jr., "Cost-effective optical waveguide components for printed circuit applications," *Proc. SPIE, Passive Compon. Fiber-Based Devices IV*, vol. 6781, p. 678116, Nov. 2007.
- [7] N. Bamiedakis, A. Hashim, J. Beals, R. V. Penty, and I. H. White, "Low-cost PCB-integrated 10-Gb/s optical transceiver built with a novel integration method," *IEEE Trans. Compon., Packag., Manuf. Technol.*, vol. 3, no. 4, pp. 592-600, Apr. 2013.
- [8] I. Papakonstantinou, D. R. Selviah, R. C. A. Pitwon, and D. Milward, "Low-cost, precision, self-alignment technique for coupling laser and photodiode arrays to polymer waveguide arrays on multilayer PCBs," *IEEE Trans. Adv. Packag.*, vol. 31, no. 3, pp. 502-511, Aug. 2008.
- [9] C. L. Schow *et al.*, "225 Gb/s bi-directional integrated optical PCB link," in *Proc. Opt. Fiber Commun. Conf. (OFC)*, Mar. 2011, pp. 1-3.
- [10] K. Schmidtke *et al.*, "960 Gb/s optical backplane ecosystem using embedded polymer waveguides and demonstration in a 12G SAS storage array," *J. Lightw. Technol.*, vol. 31, no. 24, pp. 3970-3975, Dec. 15, 2013.
- [11] P. Westbergh *et al.*, "High-speed 850 nm VCSELs with 28 GHz modulation bandwidth operating error-free up to 44 Gbit/s," *Electron. Lett.*, vol. 48, no. 18, pp. 1145-1147, Aug. 2012.
- [12] A. Larsson, "Advances in VCSELs for communication and sensing," *IEEE J. Sel. Topics Quantum Electron.*, vol. 17, no. 6, pp. 1552-1567, Nov./Dec. 2011.
- [13] D. Kuchta *et al.*, "64 Gb/s transmission over 57 m MMF using an NRZ modulated 850 nm VCSEL," in *Proc. Opt. Fiber Commun. Conf. (OFC)*, 2014, p. Th3C.2.
- [14] F. E. Doany, P. K. Pepeljugoski, A. C. Lehman, J. A. Kash, and R. Dangel, "Measurement of optical dispersion in multimode polymer waveguides," in *Proc. LEOS Summer Topical Meetings*, 2004, pp. 31-32.
- [15] P. Pepeljugoski *et al.*, "Comparison of bandwidth limits for on-card electrical and optical interconnects for 100 Gb/s and beyond," *Proc. SPIE, Optoelectron. Integr. Circuits X*, vol. 6897, p. 68970I, Feb. 2008.
- [16] T. Kosugi and T. Ishigure, "Polymer parallel optical waveguide with graded-index rectangular cores and its dispersion analysis," *Opt. Exp.*, vol. 17, no. 18, pp. 15959-15968, 2009.
- [17] T. Shiraishi, T. Yagisawa, T. Ikeuchi, S. Ide, and K. Tanaka, "Cost-effective low-loss flexible optical engine with microlens-imprinted film for high-speed on-board optical interconnection," in *Proc. IEEE 62nd Electron. Compon. Technol. Conf. (ECTC)*, May/June. 2012, pp. 1505-1510.
- [18] F. E. Doany *et al.*, "Terabit/s-class optical PCB links incorporating 360-Gb/s bidirectional 850 nm parallel optical transceivers," *J. Lightw. Technol.*, vol. 30, no. 4, pp. 560-571, Feb. 15, 2012.